Influence of carrier-carrier interaction on time-dependent intersubband absorption in a semiconductor quantum well

T. Müller, W. Parz, G. Strasser, and K. Unterrainer
Institut für Photonik und Zentrum für Mikro- und Nanostrukturen, Technische Universität Wien, A-1040 Wien, Austria
(Received 7 May 2004; published 22 October 2004)

Using ultrafast terahertz spectroscopy, we measure the temporal evolution of the intersubband absorption spectrum of a $GaAs/Al_{0.3}Ga_{0.7}As$ double-quantum-well structure with an energy spacing between the first two subbands smaller than the longitudinal optical phonon energy. We show that the interaction between the photoexcited carriers has a considerable influence on the time-dependent absorption. When varying the photoexcited sheet carrier density between 1×10^{10} cm^{-2} and more than 1×10^{12} cm^{-2}, we find (i) a strong dependence of the intersubband scattering rate on the density of optically generated carriers, and (ii) a temporal shift of the intersubband resonance as the population in the second subband decays, i.e., as the photoexcited carriers relax into the quantum-well ground state.

DOI: 10.1103/PhysRevB.70.155324 PACS number(s): 78.47.+p, 73.21.Fg, 73.50.Gr

I. INTRODUCTION

In semiconductor quantum wells (QW's) the original three-dimensional energy bands are split into so-called subbands. Optical transitions may take place between these subbands when they are partially filled with carriers,[1] which can be supplied by doping or by photoexcitation.[2] Because the subbands are parallel and the optical transitions conserve momentum, the intersubband (ISB) absorption spectrum exhibits Lorentzian-like resonances at discrete energies. In this context it is important to pose the question: What determines the resonance energy of an ISB transition? In a single-particle picture, the ISB resonance corresponds to the transition between two quantized states and is thus determined by the structural parameters of the QW. However, ISB absorption is a collective rather than a single-particle phenomenon and the many-body interaction manifests itself in a shift of the ISB resonance away from the single-particle energy spacing.[3,4] This shift not only depends on the total number of carriers in the QW but also on the distribution of the carriers in the different subbands.[5] As the second subband in a QW becomes significantly populated through strong resonant ISB excitation, for example, the ability of the carriers to screen the exciting radiation is reduced, leading to a redshift of the ISB resonance.[6]

Because a variety of novel optoelectronics devices operating in the terahertz (THz) and midinfrared spectral regime, such as quantum cascade lasers[7,8] and detectors,[9] are based on ISB transitions, a detailed understanding of their physics is of great experimental[10–13] and theoretical[14–16] interest. Many-body effects on ISB absorption spectra have been studied theoretically for the response of two-subband and multisubband QW's.[3,4,12,15,17] Experimentally, ISB transitions are usually studied by Fourier transform spectroscopy, where an infrared glow bar is used as a continuous-wave (CW) white-light source. For the measurement of carrier dynamics in QW's, pulsed excitation has to be combined with ultrashort ISB probe pulses to perform time-resolved ISB absorption spectroscopy on subpicosecond timescales. Usually, this is done by spectrally tuning midinfrared or THz probe pulses into resonance with ISB transitions and measuring the absorbed pulse energy.[18,19] The redistribution of carriers between different subbands due to relaxation, however, causes a temporal shift of the ISB resonance energies because of many-body effects. Thus, it is not sufficient in some cases (especially at high carrier densities and small subband spacings where many-body effects play an important role) to probe the time-dependent ISB absorption at a fixed energy, but instead the dynamics of the entire absorption spectrum has to be monitored. This can, for example, be achieved by replacing the CW light source of a Fourier-transform infrared spectrometer by a pulsed "white-light" THz source, where the radiation consists of only a few cycles of the electromagnetic field and therefore covers a broad spectrum. With the rapid developments in THz technology, such sources have now become available, and a new class of nonequilibrium phenomena in QW's can be studied in the THz and midinfrared spectral domain.

II. EXPERIMENT

In our experiment an interband pump pulse injects electrons into the two lowest subbands of an undoped $GaAs/Al_xGa_{1-x}As$ asymmetric double QW with a level spacing smaller than the longitudinal optical (LO)-phonon energy ($\sim$36 meV in GaAs). The time evolution of the electronic ISB absorption is monitored by probing the optical transitions to a third (empty) subband [see Fig. 1(a)]. The resulting time-dependent ISB absorption spectrum, shown schemati-

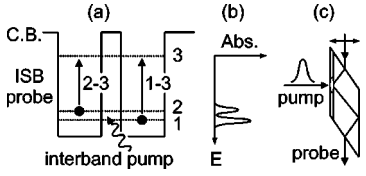

FIG. 1. (a) Energy-band diagram of the double-QW structure and (b) corresponding ISB absorption spectrum. (c) Schematic drawing of the sample geometry and pump-probe configuration.

cally in Fig. 1(b), exhibits two absorption lines, corresponding to the (2-3) and (1-3) ISB transitions, respectively. On the basis of the time evolution of the ISB absorption we determine the ISB relaxation time between subbands 1 and 2.

The undoped $GaAs/Al_{0.3}Ga_{0.7}As$ double-QW sample was grown on a 500-μm-thick semi-insulating GaAs wafer by molecular beam epitaxy. The structure contains 40 periods of a 65-Å GaAs well and a 75-Å GaAs well, coupled through a 25-Å $Al_{0.3}Ga_{0.7}As$ barrier. The separation between each pair of QW's is 200 Å. The selection rule for ISB transitions requires an electric field component perpendicular to the QW layers. Thus, the edges of the sample were polished at an angle of 58° to the growth axis, in order to form a single-pass waveguide for the ISB probe pulses [shown schematically in Fig. 1(c)] and to achieve a strong coupling of the radiation to the ISB transition dipoles. Due to the interference of the incoming and reflected wave, a standing-wave intensity pattern of the ISB-active electric field component forms along the growth direction. It is clear that the absorption strongly depends on the position of the QW's relative to the position of the intensity nodes and antinodes. Thus, the QW's were placed at a certain distance from the surface by growing a 2500-Å-thick $Al_{0.3}Ga_{0.7}As$ spacer layer on top of the sample. The sample was mounted on the cold finger of a He continuous-flow cryostat. All measurements were performed at a temperature of approximately $T=5$ K.

Time-resolved ISB absorption spectra were recorded by employing an interband-pump–ISB-probe technique, where the sample was excited from the surface [see Fig. 1(c)]. In our setup we use a mode-locked Ti:sapphire laser that delivers 12-fs pulses at a repetition rate of 75 MHz with an average output power of 800 mW. The laser pulses are centered at a wavelength of 780 nm and the bandwidth is 110 nm [full width at half maximum (FWHM)]. For interband excitation half of the laser intensity was sent through a motorized delay stage and the desired pump pulse spectrum was selected through a grating pulse shaper. The excitation energy was set slightly above the bottom of the second subband ($\sim$1.59 eV) and the spectral width was kept as small as possible (10–25 nm), in order to generate a cold electron distribution in the second subband and to suppress LO-phonon emission. Different excitation densities were achieved by changing the focus of the pump pulse at the sample and additionally by using neutral-density filters. The density of photoexcited carriers was estimated from the excitation power, repetition rate, focus diameter of the pump pulse, and the absorption coefficient of GaAs. Care was taken that the spot size of the pump was at least two times larger than that of the probe beam, so that the probe beam sampled a uniform region of photoexcitation.

The ISB probe pulses were generated by phase-matched difference frequency mixing in a 30-μm GaSe crystal.[20,21] The probe pulses were centered at a wavelength of approximately 10 μm and the pulse duration was less than 40 fs. Their large spectral width—more than 60 meV (FWHM)—allowed measuring the ISB absorption spectrum of the sample with a single pulse, offering simultaneously high resolution in both the time and frequency domains. The probe pulses were transmitted through the waveguide and detected with a liquid-nitrogen-cooled $Hg_xCd_{1-x}Te$ detector. Careful alignment of the optics allowed achieving a (diffraction-limited) 30-μm focus diameter (FWHM) of the ISB probe pulses at the position of the sample. A small probe spot diameter is desirable for two reasons. First, a small interaction volume with the pump beam improves the time resolution of the experiment. Second, a small probe spot allows us to reduce the pump spot diameter accordingly to achieve high ($>10^{12}$ cm^{-2}) photoexcited carrier densities.

Spectroscopic measurements of the probe pulses were performed by using an interferometric correlation technique. This method relies on the generation of two identical ISB probe pulses by using a sequence of two near-infrared laser pulses separated by a variable time delay. The Fourier transform of the interference signal as a function of the time delay provides the spectrum. Experimental details of this technique have been reported elsewhere.[22]

The temporal changes in the ISB absorption spectrum were obtained by a lock-in technique as a function of time delay between the interband pump and the ISB probe pulses. The data are typically presented in the form of normalized differential transmission given by $\Delta T/T_0=(T-T_0)/T_0$, the change in the transmission $\Delta T=T-T_0$ induced by the pump pulse (chopping the near-infrared pump beam) divided by the transmission of the probe without pump T_0 (chopping the probe beam).

III. RESULTS AND DISCUSSION

A. Intersubband absorption spectra

1. Low excitation density

Time-resolved ISB absorption spectra, recorded at an extremely low photoexcited sheet carrier density of $n_S=1\times10^{10}$ cm^{-2}, are shown in Fig. 2(a). The spectra exhibit absorption peaks at energies of $E_{32}=112$ meV and $E_{31}=126$ meV, corresponding to the (2-3) and the (1-3) ISB absorption, respectively. These values are in perfect agreement with the transition energies obtained by solving the single-particle Schrödinger equation in the envelope function formalism, where we used 75 and 64 Å for the GaAs well widths and 24 Å for the $Al_{0.3}Ga_{0.7}As$ barrier width in order to match the calculated energies to the experimental results. The amplitude of the low-energy peak decreases with the time delay after excitation due to ISB relaxation. The amplitude of the second peak, however, rises slightly in the beginning and afterwards decays due to carrier recombination.

Since the spectrally integrated absorption (i-3) ($i=1,2$) is directly proportional to the subband population $N_i(t)$, we are able to determine the population dynamics in the QW on the basis of the time-resolved ISB absorption spectra. Figure 2(b) shows the electron population in the first and the second subband as a function of the time-delay after optical excitation (symbols). About 40% of the photoexcited electrons are injected into the second subband, while the remaining 60% are injected into the first subband at higher k values. The population in the second subband shows exponential decay. The electrons that relax down add to the population in the ground level. Subsequently, the population in the ground level drops because of carrier recombination. The lines in the

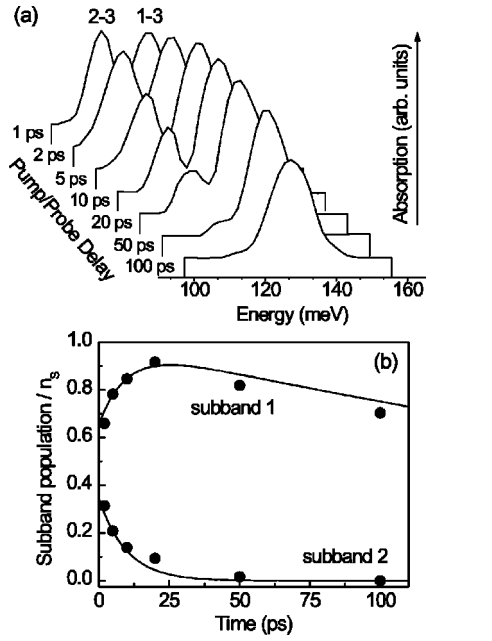

FIG. 2. (a) ISB absorption spectra at different time delays after the interband pump pulse for an excitation density of $n_S = 1 \times 10^{10}$ cm^{-2}. (b) Electron populations in subbands 1 and 2 as a function of time delay after the excitation (symbols, experiment; lines, results from a phenomenological rate-equation model).

inset of Fig. 2(b) are the results obtained from a phenomenological rate-equation model. By fitting the calculation to the experimental data we deduce an ISB relaxation time of $T_{21} = 14$ ps and a recombination time of $T_{\mathrm{rec}} \sim 0.5$ ns.

2. High excitation density

At higher excitation densities ISB transitions reveal their collective nature. Figure 3(a) shows absorption spectra taken at an excitation density of $n_S = 3 \times 10^{11}$ cm^{-2}. The spectra are vertically displaced for clarity. Compared to the low excitation density spectra, shown in Fig. 2(a), we find two differences: First, the (2-3) absorption decays much faster and we extract an ISB relaxation time of only $T_{21} = 5.9$ ps. Second,

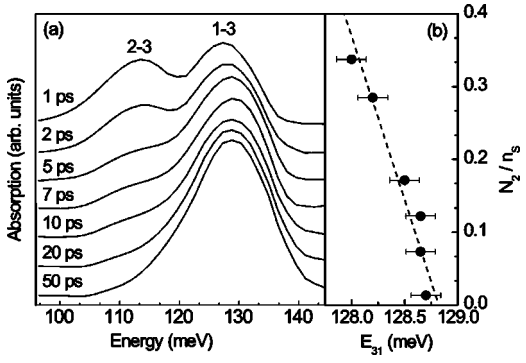

FIG. 3. (a) ISB absorption spectra at different time delays after the interband pump pulse for an excitation density of $n_S = 3 \times 10^{11}$ cm^{-2}. (b) Energetic position of the (1-3) ISB resonance as a function of the electron population in the second subband.

we observe a spectral blueshift of the (1-3) ISB absorption as the time evolves, i.e., as the electrons in the second subband relax into the QW ground level. Note that in addition to the ISB resonances we observe a monotonic absorption that increases towards low energy. This absorption is also present when we set the polarization of the ISB probe pulses parallel to the QW layers. Thus, it is attributed to Drude absorption by free carriers that are generated in the substrate, and we subtracted it for clarity. In Fig. 3(b) we plot the peak energy E_{31} of the (1-3) transition versus the carrier density N_2 in the second subband. We find that (within the accuracy of our experiment) the energetic shift of E_{31} is linear. Unfortunately, we cannot determine the exact energy shift of the (2-3) ISB transition because of its small amplitude at delay times >5 ps. Similar results have recently been obtained by Shtrichman *et al.*, who measured the time-dependent ISB absorption in a rectangular QW after photoexcitation.[23] They observed a time-dependent shift of the (1-2) ISB resonance as the density of carriers decayed due to recombination. This was explained by a density-functional model accounting for static and dynamic many-body effects.

Although in our experiment the total sheet carrier density n_S in the QW does not alter significantly during the relaxation, it is plausible that the redistribution of carriers in the two lowest subbands due to ISB relaxation can lead to energetic shifts of the ISB resonances. Qualitatively, these shifts can be understood as follows: The depolarization shift of a transition from subband 1 to 3, for example, is proportional to N_1, the population in the first subband. Thus, as the population in 1 increases, one would expect an energetic shift of the resonance to higher energy. Other many-body effects, such as exchange and correlation, will also contribute. In order to quantify these energy shifts, we applied the density functional model of Ref. 23 to calculate time- and density-dependent ISB absorption spectra of our structure. Within this model the static effects are separated into the Hartree term and the exchange-correlation term. The Hartree potential arises from the different spatial distributions of electrons in the conduction band and holes in the valence band. It was accounted for by a self-consistent solution of Schrödinger's equation and Poisson's equation. The exchange-correlation potential, which can be described as a functional of the carrier density, was added in the Schrödinger equation, in a way similar to the Hartree potential. We calculated the self-consistent static band structure of the QW for different fractions of electrons in the second subband.

We did not consider hole redistribution, i.e., we assumed a thermalized distribution of holes in their ground state for all time delays after excitation. This is justified because it is known that holes relax much faster than electrons, because of their large effective mass and the small energy spacing in the valence band. With the static self-consistent wave functions and subband energy levels from above, we then calculated the dynamic many-body corrections to the ISB absorption spectrum using the formalism described, for example, in Ref. 17. The dynamic corrections consist of the depolarization shift, which essentially comes from a time-dependent Hartree term, and the exciton interaction, which is due to the Coulomb interaction between the excited electron and the quasihole left behind in the ground subband. Dynamic inter-

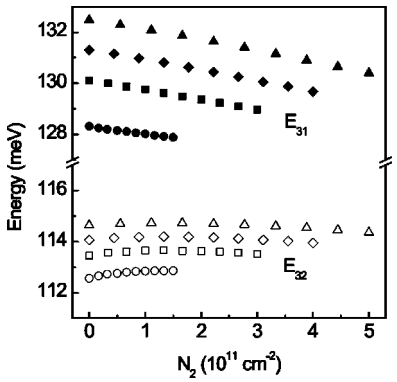

FIG. 4. Calculated energies of the (1-3) and (2-3) ISB resonances for total sheet carrier densities of $n_S = 3 \times 10^{11}$ cm^{-2} (circles), 6×10^{11} cm^{-2} (squares), 8×10^{11} cm^{-2} (diamonds), and 1×10^{12} cm^{-2} (triangles).

actions between electrons in the conduction band and holes in the valence band have been shown to be small in practically relevant cases[23] and were thus neglected.

The calculated energetic positions E_{31} and E_{32} of the (1-3) and (2-3) ISB resonances at different sheet carrier densities n_S are shown in Fig. 4. As the number of electrons in the second subband is reduced, i.e., as the electrons relax into the QW ground state, the (1-3) transition shifts to higher energy. This is in agreement with the experimental results. The magnitude of the shift is larger for higher excitation density. The energetic position of the (2-3) absorption is more stable for all excitation densities. A detailed analysis of the individual contributions of the different many-body corrections to the (1-3) ISB resonance E_{31} with respect to the single-particle energy splitting shows that the blueshift is manly due to the depolarization effect. The static Hartree term, which often dominates the many-body corrections in modulation-doped nanostructures, is minimized due to the presence of holes in the valence band.

B. Intersubband Relaxation: Excitation density dependence

In Fig. 5(a) we present the excitation density dependence of the ISB relaxation time T_{21} when varying the photoexcited sheet carrier density from $n_S = 1 \times 10^{10}$ cm^{-2} to more than 1×10^{12} cm^{-2}. With increasing density we observe a significant shortening of the relaxation time. In the high-density regime we observe a steep increase of T_{21}. In order to find the physical mechanism behind the ISB relaxation we will now discuss possible scattering mechanisms and compare numerical estimates of scattering times with the experimental results.

Since the energy spacing between the two lowest subbands of our QW structure is smaller than the LO-phonon energy, the electrons in the second subband do not possess sufficient energy to emit LO phonons, and ISB relaxation can only be due to acoustic phonon emission and carrier-carrier scattering. Using the model described in Ref. 24 we calculated the acoustic phonon scattering time to be $T_{21} \sim 0.3$ ns for our structure. This time is much too long to explain the experimental findings. Former time-resolved photoluminescence experiments[25,26] and calculations,[27] however, have shown that the ISB carrier-carrier scattering rates can be very high, almost approaching in some circumstances the ISB scattering rate due to LO-phonon emission.

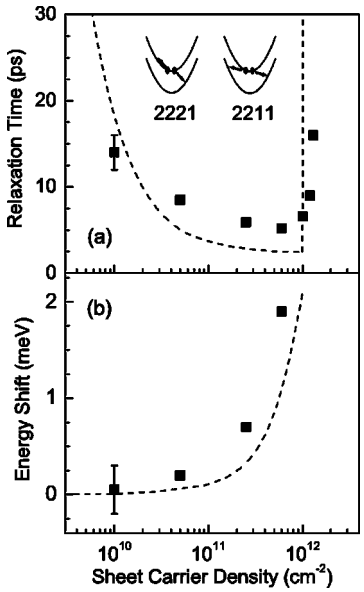

FIG. 5. (a) Experimental ISB relaxation times (symbols). The calculation (dashed line) confirms the experimental results. (b) Maximum energy shift of the (1-3) ISB resonance.

We calculated the carrier-carrier scattering rates in the Born-approximation using static single subband screening within the random phase approximation.[28] In this calculation, Pauli blocking of the final states was not taken into account. We find that the most prominent scattering processes are labeled 2211 and 2221 [see inset in Fig. 5(a)], where $ijfg$ describes an interaction, where an electron in subband i scatters to f under collision with a second electron, which scatters from j to g. When working out the total population transfer rate between the first and second subbands, both scattering processes and the number of electrons that are transferred by each process were taken into account: $T_{21} = (2W_{2211} + W_{2221})^{-1}$. The result of this calculation is shown in Fig. 5(a) as dashed line. At an excitation density of approximately 1×10^{12} cm^{-2} the Fermi level in the ground state approaches the bottom of the second subband and the ISB relaxation drastically slows down due to Pauli blocking. This is illustrated in Fig. 5(a) by the vertical dashed line. Although we cannot completely exclude the contribution of LO-phonon scattering of hot electrons in the second subband of the QW to the relaxation, the strong dependence of the ISB relaxation time T_{21} on the carrier density and the good agreement with the calculation suggest that the main relaxation mechanism is carrier-carrier scattering.

Figure 5(b) shows the maximum shift of the (1-3) ISB absorption as a function of the excitation density. The theoretical density dependence of the (1-3) peak shift, calculated as described above, is shown as a dashed line. The many-body corrections are rather small in our case—less than 2% of the bare energy spacing. However, having in mind that the depolarization shift of an ISB transition (i-j) is a function of $(E_j - E_i)^{-1}$, it is clear that the collective effects can become

substantial when probing ISB transitions with a subband separation in the THz spectral range (in the order of 10 meV). Monitoring the ISB absorption at a fixed energy might then give erroneous results.

In an ordinary ensemble of two-level systems the transition energy—and thus the interaction strength between particles (e.g., carrier-phonon interaction or carrier-carrier interaction)—does not depend on the excited-state population. In a highly excited QW structure, however, many-body effects influence the energy spacing dependent on the populations in the two subbands. Thus, as electrons relax into the ground state the interaction strength between particles is altered, which in turn influences the relaxation rate. This leads to a complicated interplay between many-body effects and the physical processes that cause the relaxation. Therefore, ISB relaxation of carriers in a highly excited QW structure is a complicated problem that is described by a single time constant only to first order.

IV. SUMMARY AND CONCLUSION

In conclusion, we have investigated the infrared optical properties and relaxation dynamics of photoexcited electrons in a $GaAs/Al_xGa_{1-x}As$ double-QW structure by interband-pump–ISB-probe spectroscopy. We have presented time-resolved ISB absorption spectra for a wide range of excitation densities. From the data we have extracted the density dependence of the ISB relaxation time T_{21}. Due to the small energy spacing between the two lowest subbands, LO-phonon scattering is suppressed and we have found that ISB relaxation in this structure is mainly due to carrier-carrier scattering. Further, we have shown that the ISB absorption and relaxation do not depend only on the total number of carriers in the QW but also on their distribution in the different subbands. We have observed a temporal shift of the (1-3) ISB resonance as the population in the second subband decays, i.e., as the electrons relax into the QW ground level. This has been explained by a density-functional model accounting for static and dynamic many-body effects.

ACKNOWLEDGMENTS

The authors would like to acknowledge financial support from the Austrian "Fond zur Förderung der Wissenschaftlichen Forschung" (SFB-ADLIS, START Y-47) and the EU-NMP-Project ANSWER.

[1] *Intersubband Transitions in Quantum Wells I and II*, edited by H. C. Liu and F. Capasso, Vols. 62 and 66 of Semiconductors and Semimetals (Academic Press, San Diego, 2000).
[2] M. Olszakier, E. Ehrenfreund, E. Cohen, J. Bajaj, and G. J. Sullivan, Phys. Rev. Lett. **62**, 2997 (1989).
[3] S. J. Allen, D. C. Tsui, and B. Vinter, Solid State Commun. **20**, 425 (1976).
[4] T. Ando, Z. Phys. B **26**, 263 (1977).
[5] D. Huang, G. Gumbs, and M. O. Manasreh, Phys. Rev. B **52**, 14 126 (1995).
[6] K. Craig, B. Galdrikian, J. N. Heyman, A. G. Markelz, J. B. Williams, M. S. Sherwin, K. Campman, P. F. Hopkins, and A. C. Gossard, Phys. Rev. Lett. **76**, 2382 (1996).
[7] J. Faist, F. Capasso, D. L. Sivco, C. Sirtori, A. L. Hutchinson, and A. Y. Cho, Science **264**, 553 (1994).
[8] R. Köhler, A. Tredicucci, F. Beltram, H. E. Beere, E. H. Linfield, A. G. Davies, D. A. Ritchie, R. C. Iotti, and F. Rossi, Nature (London) **417**, 156 (2002).
[9] B. F. Levine, J. Appl. Phys. **74**, R1 (1993).
[10] C. W. Luo, K. Reimann, M. Woerner, T. Elsaesser, R. Hey, and K. H. Ploog, Phys. Rev. Lett. **92**, 047402 (2004).
[11] G. B. Serapiglia, E. Paspalakis, C. Sirtori, K. L. Vodopyanov, and C. C. Phillips, Phys. Rev. Lett. **84**, 1019 (2000).
[12] R. J. Warburton, K. Weilhammer, J. P. Kotthaus, M. Thomas, and H. Kroemer, Phys. Rev. Lett. **80**, 2185 (1998).
[13] D. Dini, R. Köhler, A. Tredicucci, G. Biasiol, and L. Sorba, Phys. Rev. Lett. **90**, 116401 (2003).
[14] A. A. Batista, P. I. Tamborenea, B. Birnir, M. S. Sherwin, and D. S. Citrin, Phys. Rev. B **66**, 195325 (2002).
[15] C. A. Ullrich and G. Vignale, Phys. Rev. Lett. **87**, 037402 (2001).
[16] M. Zaluzny, Phys. Rev. B **47**, 3995 (1993).
[17] L. Brey, J. Dempsey, N. F. Johnson, and B. I. Halperin, Phys. Rev. B **42**, 1240 (1990).
[18] J. N. Heyman, K. Unterrainer, K. Craig, J. Williams, M. S. Sherwin, K. Campman, P. F. Hopkins, A. C. Gossard, B. N. Murdin, and C. J. G. M. Langerak, Appl. Phys. Lett. **68**, 3019 (1996).
[19] B. N. Murdin, W. Heiss, C. J. G. M. Langerak, S.-C. Lee, I. Galbraith, G. Strasser, E. Gornik, M. Helm, and C. R. Pidgeon, Phys. Rev. B **55**, 5171 (1997).
[20] R. A. Kaindl, D. C. Smith, and T. Elsaesser, Opt. Lett. **23**, 861 (1998).
[21] R. Huber, A. Brodschelm, F. Tauser, and A. Leitenstorfer, Appl. Phys. Lett. **76**, 3191 (2000).
[22] T. Müller, R. Bratschitsch, G. Strasser, and K. Unterrainer, Appl. Phys. Lett. **79**, 2755 (2001).
[23] I. Shtrichman, C. Metzner, E. Ehrenfreund, D. Gershoni, K. D. Maranowski, and A. C. Gossard, Phys. Rev. B **65**, 035310 (2001).
[24] R. Ferreira and G. Bastard, Phys. Rev. B **40**, 1074 (1989).
[25] M. Hartig, S. Haacke, P. E. Selbmann, B. Deveaud, R. A. Taylor, and L. Rota, Phys. Rev. Lett. **80**, 1940 (1998).
[26] M. Hartig, J. D. Ganière, P. E. Selbmann, B. Deveaud, and L. Rota, Phys. Rev. B **60**, 1500 (1999).
[27] K. Kempa, P. Bakshi, J. Engelbrecht, and Y. Zhou, Phys. Rev. B **61**, 11 083 (2000).
[28] J. H. Smet, C. G. Fonstad, and Q. Hu, J. Appl. Phys. **79**, 9305 (1996).